

ELECTROMAGNETIC PROTON/PROTON INSTABILITY AND ITS IMPLICATIONS FOR ION HEATING IN THE EXTENDED FAST SOLAR WIND

XINLIANG GAO¹, QUANMING LU¹, XING LI², LICAN SHAN¹, AND SHUI WANG¹

¹ CAS Key Laboratory of Geospace Sciences, Department of Geophysics and Planetary Science,
University of Science and Technology of China, Hefei 230026, China; qmlu@ustc.edu.cn

² Institute of Mathematics and Physics, Aberystwyth University, Aberystwyth SY23 3BZ, UK

Received 2012 July 16; accepted 2012 December 13; published 2013 January 28

ABSTRACT

Two-dimensional hybrid simulations are performed in this paper to investigate the proton/proton instability in low beta plasma. The obliquely propagating Alfvén waves are found to be unstable to the proton/proton instability. At first, the Alfvén waves have a nearly linear polarization, and both the ambient protons and minor ions O⁶⁺ can be resonantly heated. The heating is primarily in the direction perpendicular to the background magnetic field. With the evolution of the instability, the obliquely propagating Alfvén waves gradually become left-hand polarized, and then cannot resonantly heat the ambient protons or minor ions O⁶⁺. The effects of the plasma beta and temperature anisotropy of the ambient protons on the evolution of the instability are also studied in this paper. Finally, the implications of our simulation results for ion heating in the extended fast solar wind are discussed.

Key words: methods: numerical – solar wind – waves

Online-only material: color figure

1. INTRODUCTION

In situ plasma measurements of proton velocity distributions in the fast solar wind ($V_{sw} \geq 600$ km/s) have revealed that besides an ambient component there typically exists a separate beam or a secondary component streaming away from the Sun along the ambient magnetic field, \mathbf{B}_0 (Feldman et al. 1973, 1974; Goodrich & Lazarus 1976; Marsch et al. 1982; Marsch 1991; Goldstein et al. 2000; Tu et al. 2004). Helios observations reported by Marsch & Livi (1987) show the relative velocity between the ambient and beam protons (U_{ab}) satisfies $0 < U_{ab}/V_A \leq 3$, where V_A represents the local Alfvén speed. Later, Goldstein et al. (2000) illustrated that $0 < U_{ab}/V_A \leq 2$ through the measurements made by the *Ulysses* SWOOPS instrument. The minor ions in the fast solar wind are also found to stream faster than the ambient protons with a relative drifting speed of about one local Alfvén speed (Marsch et al. 1982; von Steiger et al. 1995; von Steiger & Zurbuchen 2006), and they are always preferentially heated and have a higher temperature with $T_i \geq A_i T_p$ (von Steiger et al. 1995; Marsch 2006; where T_i and T_p are the temperature of ion species i and protons, respectively, and A_i is the atomic mass number of ion species i).

Besides the double-peak proton velocity distributions, another pervasive feature in the fast solar wind is the marked temperature anisotropy of the ambient protons with a larger perpendicular temperature than the parallel temperature ($T_{a\perp}/T_{a\parallel} > 1$). Such a temperature anisotropy of the ambient protons was first discovered near 1 AU in the early days of space probes (Feldman et al. 1974). Later, *Helios* observations indicated that the temperature anisotropy of the ambient protons, $T_{a\perp}/T_{a\parallel}$, is high and about 3–4 in the high-speed wind near 0.3 AU (Marsch et al. 1982). A large temperature anisotropy of protons and oxygen ions with $T_{\perp}/T_{\parallel} > 1$ also exists in the near Sun region above coronal holes (Kohl et al. 1998; Li et al. 1998), where the plasma beta is much smaller than unity. The average dependence of the proton temperature on heliocentric radial distance R can be given by a power law $R^{-\alpha}$, where $\alpha \simeq 1$

for $T_{\parallel a}$ and $0.7 < \alpha < 1$ for $T_{a\perp}$ (Marsch et al. 1982). Obviously, the observed temperature anisotropy does not agree with the strict adiabatic expansion, which would bring about a parallel temperature much larger than the perpendicular temperature near 1 AU. Thus, the local heating of protons must be taken into consideration as the fast solar wind travels in the interplanetary space. However, until now, there is no consensus on the physical process capable of explaining the heating of the ambient protons and their temperature anisotropy. Some possible sources include the cascade of turbulence (Cranmer 2002; Hollweg & Isenberg 2002; Araneda et al. 2008, 2009; Valentini & Veltri 2009; Valentini et al. 2010), quasi-perpendicular interplanetary shocks (Gosling et al. 1984; Ofman et al. 2009), and the instabilities driven by interplanetary pick-up ions (Gray et al. 1996; Richardson et al. 1996).

In this paper, we propose that the free energy of the beam protons in the extended fast solar wind may provide one of the possible sources of ion heating. With two-dimensional (2D) hybrid simulations, we study the electromagnetic proton/proton instability in low beta plasma. The ambient protons, as well as the minor ions O⁶⁺, can be effectively heated by the obliquely propagating Alfvén waves excited by the proton/proton instability, and they are preferentially heated in the perpendicular direction. The implications of our simulation results to ion heating in the extended fast wind are also discussed. The characteristics of the excited waves from proton/proton instability have already been extensively studied by both the linear Vlasov theory and hybrid simulations (Gary 1991; Gary et al. 1993; Daughton & Gary 1998; Daughton et al. 1999; Li & Lu 2010). In low beta plasma, the oblique Alfvén waves are found to have a lower threshold, while the parallel magnetosonic waves have a lower threshold in high beta plasma (Daughton & Gary, 1998; Daughton et al. 1999; Gary et al. 2000; Lu et al. 2009).

The organization of this paper is as follows. Section 2 describes the plasma parameters and simulation model. The simulation results are illustrated in Section 3. A summary and discussions are presented in Section 4.

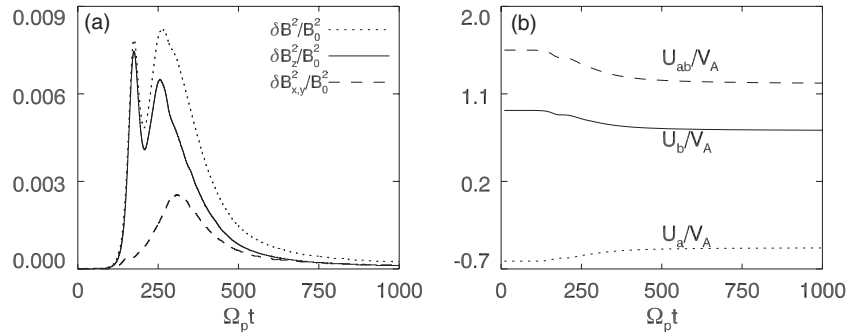


Figure 1. Time evolution of (a) the amplitude of the fluctuating magnetic field $\delta B^2/B_0^2$, $\delta B_{x,y}^2/B_0^2$ (where $\delta B_{x,y}^2 = \delta B_x^2 + \delta B_y^2$), and $\delta B_z^2/B_0^2$, (b) the bulk velocities of the beam (U_b/V_A) and ambient protons (U_a/V_A), and the relative speed between them (U_{ab}/V_A) for Run 1.

Table 1
Some Parameters for Different Simulation Runs

Run	$\beta_{a\parallel}$	$T_{a\perp}/T_{a\parallel}$
Run 1	0.01	1.0
Run 2	0.02	1.0
Run 3	0.1	1.0
Run 4	0.01	0.5
Run 5	0.01	2.0

2. SIMULATION MODEL

A 2D hybrid simulation model with periodic boundary condition is used to study the electromagnetic proton/proton instability in low beta plasma. In hybrid simulations, the ions are treated kinetically with the standard particle-in-cell method, while the electrons are treated as massless fluid (Winske 1985; Quest 1988; Winske & Omidi 1993; Lu et al. 2009). We divided the protons into two parts, the ambient protons and the beam protons, according to the double-peak velocity distribution of protons observed in the fast solar wind. Five runs are performed. The parallel plasma beta and temperature anisotropy of the ambient protons for each run are shown in Table 1. According to the linear theory, only the obliquely propagating Alfvén waves are excited in these situations (Daughton & Gary 1998).

For all runs, the beam protons initially have an isotropic Maxwellian distribution with a drift velocity along the background magnetic field. Their temperature is the same as the parallel temperature of the ambient protons. The electron distribution is isotropic here and their temperature is the same as that of the ambient protons. The number density of the beam component is chosen as $n_b = 0.4n_e$, which is a reasonable value according to the statistical observations by *Ulysses* (Goldstein et al. 2000). Initially, the relative velocity U_{ab} between the beam protons and ambient protons is parallel to the background magnetic field $\mathbf{B}_0 = B_0\hat{x}$. U_{ab} is set to be $1.55V_A$, which is a little bit larger than the local Alfvén speed. In Run 1, we also study the dynamics of the minor ions O^{6+} , which are the most abundant heavy ions in the solar wind (von Steiger et al. 2000) during the evolution of the instability. Here, O^{6+} is treated as a test particle for its low density, and its thermal velocity is the same as that of the ambient protons. The relative speed between the ambient protons and the oxygen ions is set to be $1.22V_A$ which is parallel to the ambient magnetic field.

The number of grid cells is $n_x \times n_y = 512 \times 256$, and the grid cell size is $\Delta x = \Delta y = 0.8c/\omega_{pp}$ (where c/ω_{pp} is the proton inertial length). The electron resistive length is set as $L_r = \eta c^2/(4\pi v_A) = 0.02c/\omega_{pp}$. There are an average of 100

macroparticles in every cell for each species. The simulations are performed in the center-of-mass frame, where the charge neutrality ($\sum_j e_j n_j = 0$, where j denotes the species of particles) and the zero current condition ($\sum_j e_j n_j V_{0j} = 0$) are satisfied initially. The time step is $\Omega_p \Delta t = 0.025$.

3. SIMULATION RESULTS

Figure 1 displays the time evolution of (a) the amplitude of the fluctuating magnetic field $\delta B^2/B_0^2$, $\delta B_{x,y}^2/B_0^2$ (where $\delta B_{x,y}^2 = \delta B_x^2 + \delta B_y^2$) and $\delta B_z^2/B_0^2$, (b) the bulk velocities of the beam and ambient protons, and the relative speed between them for Run 1. The instability begins to be excited at $\Omega_p t \approx 125$, then the amplitude of the fluctuating magnetic field increases. The instability saturates at $\Omega_p t \approx 270$ with the amplitude of $\delta B^2/B_0^2 \approx 0.0082$. We can also find that the amplitude of $\delta B_z^2/B_0^2$ is much larger than that of $\delta B_{x,y}^2/B_0^2$ before $\Omega_p t \approx 350$. Because our simulations are performed at the $x - y$ plane, and the wavevectors of the excited waves are also limited to the same plane, this means that the excited Alfvén waves have a nearly linear polarization (such linear polarization is predicted by the linear theory; see Li & Lu 2010). However, the amplitude of $\delta B_{x,y}^2/B_0^2$ increases after $\Omega_p t \approx 250$ until it is almost the same as that of $\delta B_z^2/B_0^2$ after $\Omega_p t \approx 600$, and the waves are changed to be left-hand polarized. With the excitation of the waves, the beam protons are decelerated while the ambient protons are accelerated slightly. As a result, the relative bulk speed between the two components decreases with the excitation of the instability, and it reduces to about $1.21V_A$ after the saturation of the instability.

Figure 2 shows (a) the contour plot of the fluctuating magnetic field along the z -direction $\delta B_z/B_0$ and (b) the characteristics of the $k_x - k_y$ diagram obtained from the fast Fourier transform (FFT) of $\delta B_z/B_0$ at different times for Run 1. The obliquely propagating waves can be easily observed in Figure 2(a). The propagating angle $\theta = \arctan(k_y/k_x)$ has a definite range, and it becomes smaller during the nonlinear evolution. At $\Omega_p t = 150$, 250, and 700 the ranges of the propagating angle are about from 35° to 60° , 20° to 51° , and 27° to 43° , respectively. Meanwhile, the wavenumbers also become smaller during the evolution. The results are consistent with the work of Lu et al. (2009). This result provides the evidence that the excited Alfvén waves are indeed oblique to the ambient magnetic field because the perpendicular wavenumbers are comparable to or even larger than the parallel one. The propagating angle of the dominant mode (the mode with the maximum amplitude) at $\Omega_p t = 150$, 250, and 700 is about 50° , 40° , and 34° , respectively.

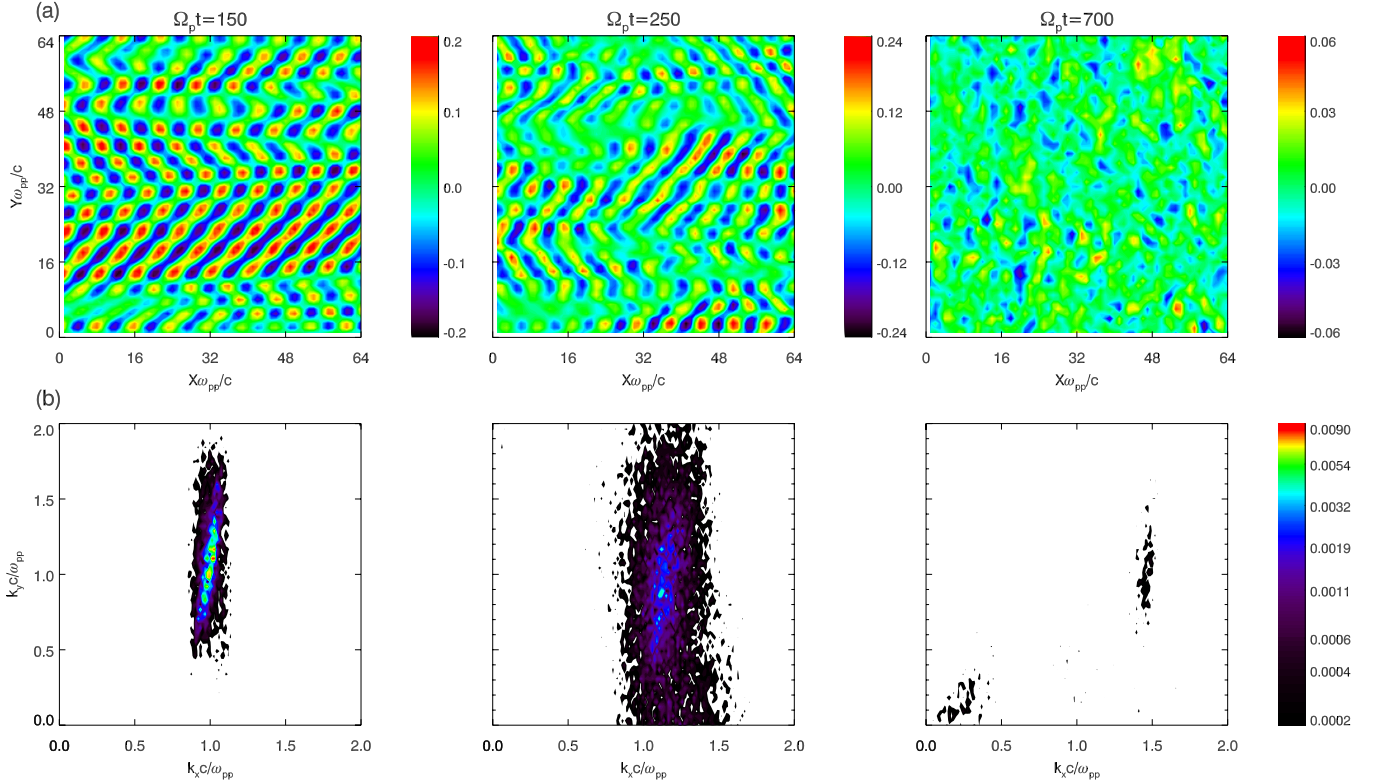


Figure 2. (a) Contour plot of the fluctuating magnetic field along the z -direction $\delta B_z/B_0$ and (b) the contour of characteristics of the $k_x - k_y$ diagram obtained from the fast Fourier transform (FFT) of $\delta B_z/B_0$ at $\Omega_p t = 150, 250,$ and 700 for Run 1.

(A color version of this figure is available in the online journal.)

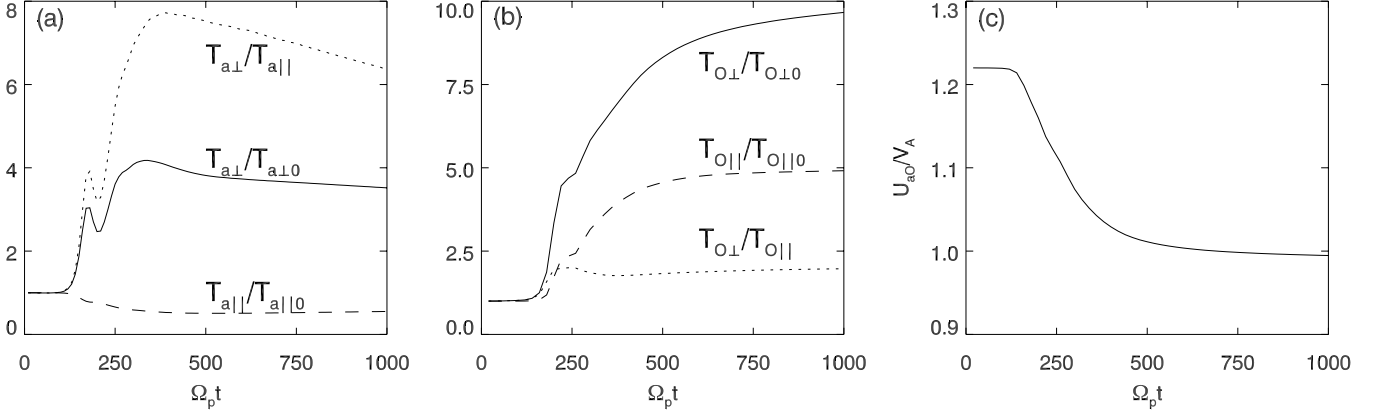


Figure 3. Time evolution of (a) the parallel temperature $T_{a\parallel}/T_{a\parallel 0}$, the perpendicular temperature $T_{a\perp}/T_{a\perp 0}$, and temperature anisotropy $T_{a\perp}/T_{a\parallel}$ of the ambient protons; (b) the parallel temperature $T_{O\parallel}/T_{O\parallel 0}$, the perpendicular temperature $T_{O\perp}/T_{O\perp 0}$, and temperature anisotropy $T_{O\perp}/T_{O\parallel}$ of minor ions O^{6+} ; and (c) the relative speed between the ambient protons and oxygen ions U_{aO}/V_A for Run 1.

The time evolution of (a) the temperatures of the ambient protons, (b) the temperatures of the minor ions O^{6+} , and (c) the relative speed between the ambient protons and oxygen ions for Run 1 are shown in Figure 3. The parallel and perpendicular temperatures are calculated using the following procedure: we first calculate the parallel temperature $T_{j\parallel} = (m_j/k_B)\langle(v_x - \langle v_x \rangle)^2\rangle$ and the perpendicular temperature $T_{j\perp} = (m_j/2k_B)\langle(v_y - \langle v_y \rangle)^2 + (v_z - \langle v_z \rangle)^2\rangle$ for ion species j in every grid cell (the bracket $\langle \bullet \rangle$ denotes an average over one grid cell), and then the temperatures are averaged over all grids. Using this method, the effects of the bulk velocity at each location on the thermal temperature can be eliminated (Lu et al. 2009; Lu & Chen 2009). From Figures 3(a) and (b), we

find that with the excitation of waves both the ambient protons and O^{6+} can be heated, mainly in the perpendicular direction. At the quasi-equilibrium stage, the parallel temperature $T_{a\parallel}/T_{a\parallel 0}$ and perpendicular temperature $T_{a\perp}/T_{a\perp 0}$ of the ambient protons are about 0.55 and 3.5. Therefore, the ambient protons obtain a large temperature anisotropy, which is about 6.4. For minor ions O^{6+} , at the end of the simulation, their parallel temperature $T_{O\parallel}/T_{O\parallel 0}$ and perpendicular temperature $T_{O\perp}/T_{O\perp 0}$ are about 4.9 and 9.7 with the temperature anisotropy about 2.0. Obviously, the heating of these minor ions is more efficient than that of the protons, which means that O^{6+} can be preferentially heated by the excited waves. The enhancement of the temperatures of the ambient protons and O^{6+} is consistent with

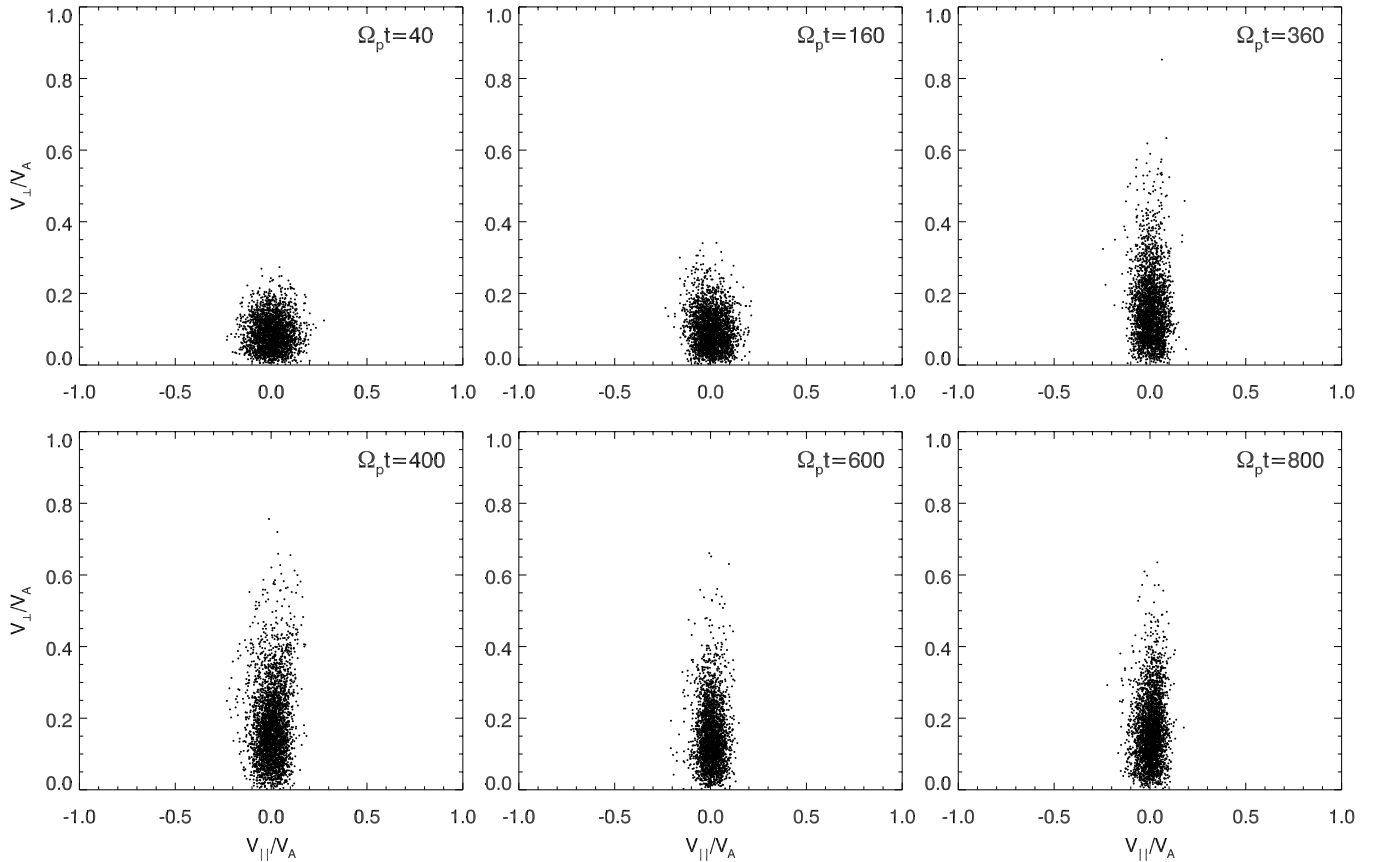


Figure 4. Scatter plots of ambient protons in the $(v_{\parallel}, v_{\perp})$ space at different times for Run 1.

the excitation of the nearly linearly polarized Alfvén waves (at $\Omega_p t \approx 125$), and the enhancement stops when the waves become left-hand polarized (at $\Omega_p t \approx 350$). It is indicated that both the ambient protons and O^{6+} can be resonantly heated by the linearly polarized Alfvén waves but have no obvious interaction with the subsequent left-hand polarized waves. At the same time, the relative speed between the ambient protons and O^{6+} decreases with the excitation of the oblique Alfvén waves and reaches about one Alfvén speed at the quasi-equilibrium stage.

The resonant interaction between the excited waves and particles can be quantitatively illustrated by the cyclotron resonant factor (Daughton & Gary 1998; Gary et al. 2000), which is $\zeta_j^{\pm} = (\omega - k_{\parallel} U_j \pm \Omega_j) / k_{\parallel} v_{j\parallel th}$ (where ω is the wave frequency, k_{\parallel} is parallel wave number. + and - represent the right-hand and left-hand polarized waves, respectively. U_j , $\Omega_j = q_j B_0 / mc$, and $v_{j\parallel th} = \sqrt{2k_B T_{j\parallel} / m_j}$ are the bulk velocity, gyro-frequency, and the parallel thermal velocity of the j th ion species). Small or intermediate values of the factor ($|\zeta| < 3$) correspond to a resonant interaction between the wave and particles (Daughton & Gary 1998; Gary et al. 2000).

We can calculate the resonant factors for both the ambient protons and minor ions O^{6+} at $\Omega_p t = 250$, when the nearly linearly polarized Alfvén waves are the dominant wave modes. A linearly polarized wave can be considered as the superposition of a left- and a right-hand polarized Alfvén wave. The frequency of the dominant wave can be obtained by calculating wavelet power spectrum of the time series of $\delta B_z / B_0$ (not shown), and other parameters can be acquired in Figures 1–3. With $\omega \approx 0.15\Omega_p$, $k_{\parallel} c / \omega_{pp} \approx 1.2$, $U_a \approx -0.563V_A$ and $v_{a\parallel th} \approx$

$0.081V_A$, we can calculate the resonant factor between the ambient protons and left-(right-) hand polarized Alfvén waves is about 1.79 (18.8). For O^{6+} , with $\omega \approx 0.15\Omega_p$, $k_{\parallel} c / \omega_{pp} \approx 1.2$, $U_O \approx 0.551V_A$, and $v_{O\parallel th} \approx 0.161V_A$, the resonant factor is about 4.6 and 0.7 for the left-hand and right-hand polarized Alfvén waves, respectively. Therefore, the ambient protons can resonantly interact with the left-hand polarized component while the O^{6+} can be resonant with the right-hand polarized component. Both the ambient protons and O^{6+} can be resonantly heated by the excited linearly polarized Alfvén waves.

The bulk velocity of the ambient protons increases after they resonantly interact with the linearly polarized Alfvén waves. Then the resonant factor between the ambient protons and the left-hand polarized component increases, and the resonant interaction stops when the excited waves become left-hand polarized after $\Omega_p t \approx 350$. Therefore, we cannot observe further heating of both the ambient protons and O^{6+} after $\Omega_p t \approx 350$. For example, at $\Omega_p t = 500$, with $\omega \approx 0.15\Omega_p$, $k_{\parallel} c / \omega_{pp} \approx 1.1$, $U_a \approx -0.496V_A$ and $v_{a\parallel th} \approx 0.071V_A$, the resonant factor of the ambient protons is about 3.9, while for O^{6+} , with $\omega \approx 0.15\Omega_p$, $k_{\parallel} c / \omega_{pp} \approx 1.1$, $U_O \approx 0.515V_A$ and $v_{O\parallel th} \approx 0.214V_A$, the resonant factors is about 3.4.

To show the heating of the protons and O^{6+} more intuitively, we illustrate the scatter plots of protons and heavy ions at different times in Figures 4 and 5. In the figures, the particles in 25 cells are recorded, and in every cell, the bulk velocity has been subtracted in order to eliminate the contribution of the bulk velocity. Both the ambient protons and O^{6+} can be scattered and heated when the excited waves have nearly linear polarization, and the scattering occurs mainly in the perpendicular direction.

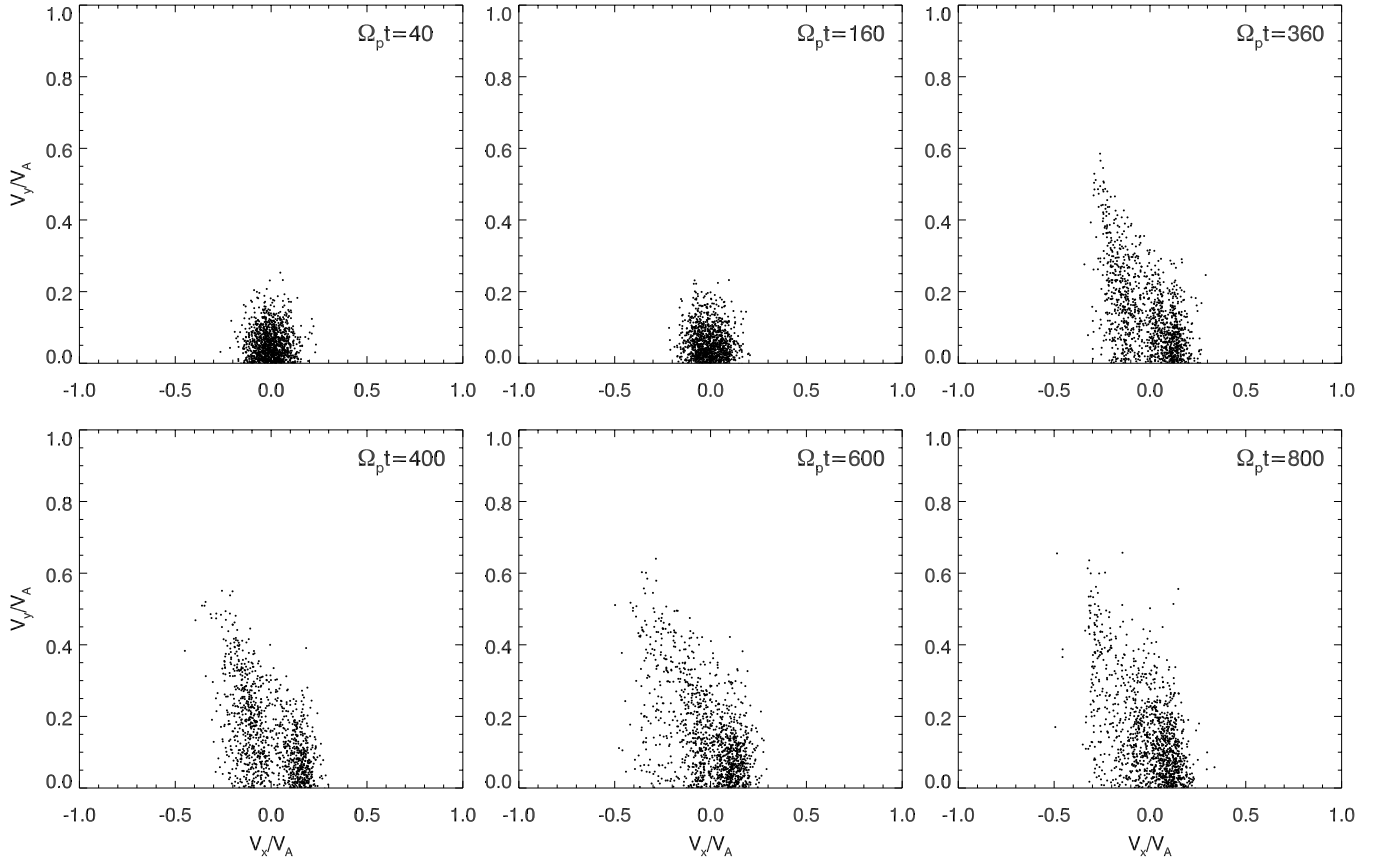


Figure 5. Scatter plots of heavy ions O^{6+} in the $(v_{||}, v_{\perp})$ space at different times for Run 1.

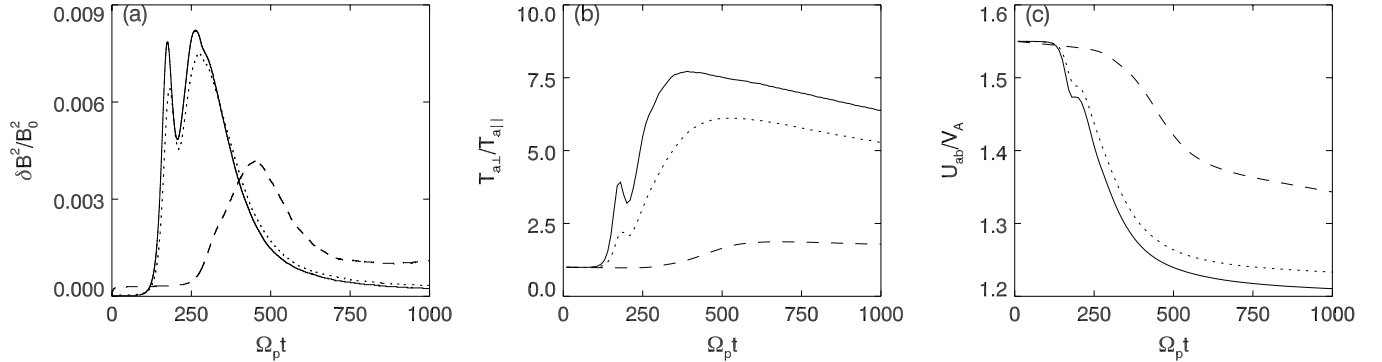


Figure 6. Time histories of (a) the amplitude of the fluctuating magnetic field $\delta B^2/B_0^2$, (b) the temperature anisotropy of ambient protons $T_{a\perp}/T_{a\parallel}$, and (c) the relative speed between beam and ambient protons U_{ab}/V_A for Runs 1, 2, and 3. The solid lines, dotted lines, and dashed lines denote the results for Runs 1, 2, and 3, respectively.

In this way, the anisotropic distributions are formed. When the waves become left-hand polarized after about $\Omega_p t = 400$, the perpendicular scattering stops because there is no obvious resonant interaction between the left-hand polarized Alfvén waves and particles.

We also study the effects of the initial parallel plasma beta and temperature anisotropy of the ambient protons on the evolution of the excited Alfvén waves, and the heating of the ambient protons and O^{6+} . Runs 2 and 3 investigate the effects of the initial plasma beta of the ambient protons, while Runs 4 and 5 consider the effects of the initial temperature anisotropy of the ambient protons. The results of Runs 1, 2, and 3 are shown in Figure 6, which plots the time evolution of (a) the amplitude of the fluctuating magnetic field $\delta B^2/B_0^2$, (b) the temperature

anisotropy of the ambient protons $T_{a\perp}/T_{a\parallel}$, and (c) the relative speed between the beam and ambient protons U_{ab}/V_A . In the figure, the solid, dotted, and dashed lines denote the results for Runs 1, 2, and 3, respectively. Through Figure 6(a), we can find that the saturated amplitude of the fluctuating magnetic field for Runs 1, 2, and 3 is about 0.0082, 0.0074, and 0.0042, respectively. At the quasi-equilibrium stage, the temperature anisotropy of the ambient protons for Runs 1, 2, and 3 is about 6.4, 5.3, and 1.8, respectively, while the relative speed between the beam and ambient protons for the three runs is $1.21V_A$, $1.23V_A$, and $1.34V_A$. Therefore, it is obvious that the increase of the initial proton plasma beta will lead to the decrease of the amplitude of excited waves and the temperature anisotropy of the ambient protons.

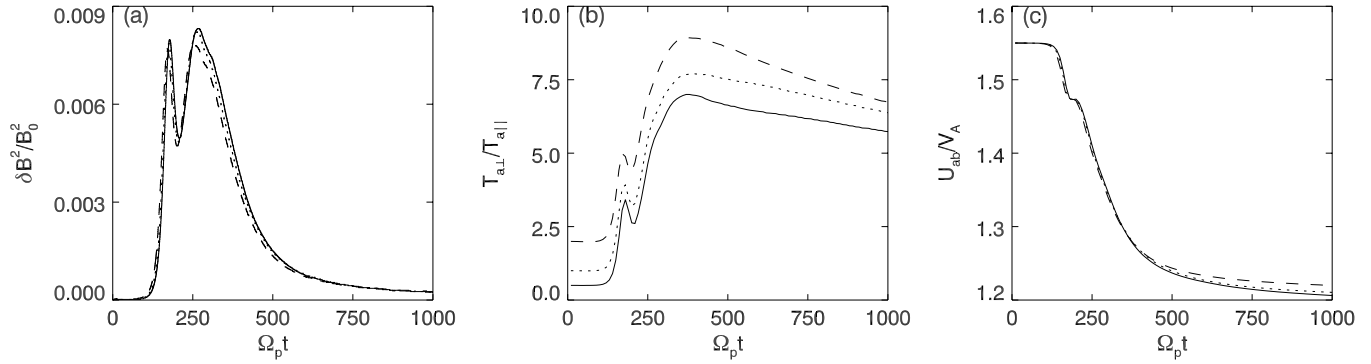


Figure 7. Time histories of (a) the amplitude of the fluctuating magnetic field $\delta B^2/B_0^2$, (b) the temperature anisotropy of ambient protons $T_{a\perp}/T_{a\parallel}$, and (c) the relative speed between beam and ambient protons U_{ab}/V_A for Runs 4, 1, and 5. The solid lines, dotted lines, and dashed lines denote the results for Runs 4, 1, and 5, respectively.

The simulation results of Runs 1, 4, and 5 are shown in Figure 7, which plots the time evolution of (a) the amplitude of the fluctuating magnetic field $\delta B^2/B_0^2$, (b) the temperature anisotropy of the ambient protons $T_{a\perp}/T_{a\parallel}$, and (c) the relative speed between the beam and ambient protons U_{ab}/V_A . In the figure, the solid, dotted, and dashed lines describe the results for Runs 4, 1, and 5, respectively. Through Figure 7(a), we can find the saturated amplitude of the fluctuating magnetic field for Runs 4, 1, and 5 is about 0.0083, 0.0082, and 0.0078. The final values of the temperature anisotropy for Runs 4, 1, and 5 are about 5.7, 6.4, and 6.7. The initial temperature of the ambient protons has little influence on the amplitude of the fluctuating magnetic field and the relative speed between the beam and ambient protons, although it can modulate the evolution of the temperature anisotropy of the ambient protons.

4. CONCLUSIONS AND DISCUSSION

By employing 2D hybrid simulations, the nonlinear evolution of the obliquely propagating Alfvén waves excited by the electromagnetic proton/proton instability in low beta plasma is investigated. At first, the oblique Alfvén waves with a nearly linear polarization begin to grow. The waves can resonantly heat both the ambient protons and O^{6+} , and O^{6+} is preferentially heated. The heating is primarily in the direction perpendicular to the background magnetic field, therefore, both the ambient protons and O^{6+} have a large temperature anisotropy. The Alfvén waves tend to become left-hand polarized gradually and at last neither the ambient protons nor O^{6+} can be resonantly heated. We also find that the increase of the initial plasma beta of the ambient protons will decrease the amplitude of the oblique Alfvén waves, and then the heating efficiency of the ambient protons. At the same time, the initial temperature anisotropy of the ambient protons can modulate the evolution of the temperature anisotropy, however, it has no obvious effects on the evolution of the amplitude of the excited waves and the relative speed between the beam and ambient components.

The heating of minor ions with a drift speed by linearly polarized obliquely propagating Alfvén waves in the extended fast solar wind has already been investigated by Li & Lu (2010) with one-dimensional (1D) hybrid simulations, and the waves are also excited by the proton/proton instability. In their simulations, a medium plasma beta of the ambient protons $\beta_{a\parallel} = 0.3$ is used, and they also suggested that the minor ions are resonantly heated by the right-hand polarized part of the nearly linearly polarized Alfvén waves and the resonance can effectively limit the drift speed between oxygen ions and protons

to the local Alfvén speed. In this paper, with more reasonable 2D hybrid simulations, we find that the ambient protons, as well as minor ions, can be resonantly heated by the oblique Alfvén waves when the plasma beta of the ambient protons is sufficiently small, and the ambient protons are heated by the left-hand polarized part of the linearly polarized Alfvén waves.

In situ measurements of the temperature anisotropy of the ambient protons in the fast solar wind show that it does not obey the strict adiabatic expansion (Marsch et al. 1982). One or several mechanisms of the local heating must be provided to explain the temperature anisotropy of the ambient protons as the fast solar wind cruises in the interplanetary space. Our simulations show that the resonant interaction between the ambient protons and the oblique Alfvén waves excited by the proton/proton instability in the fast solar wind may provide one of the possible mechanisms for ion heating when the plasma beta of the ambient protons is sufficiently small.

This research was supported by the National Science Foundation of China under grants 41174114, 41274144, 40931053, 41121003, 973 Program (2012CB825602), CAS Key Research Program KZZD-EW-01, Ocean Public Welfare Scientific Research Project, State Oceanic Administration People’s Republic of China (No. 201005017), and the Fundamental Research Funds for the Central Universities (WK2080000010).

REFERENCES

- Araneda, J. A., Maneva, Y., & Marsch, E. 2009, *PhRvL*, **102**, 175001
Araneda, J. A., Marsch, E., & Vinas, A. F. 2008, *PhRvL*, **100**, 125003
Cranmer, S. R. 2002, *SpSR*, **101**, 229
Daughton, W., & Gary, S. P. 1998, *JGR*, **103**, 20613
Daughton, W., Gary, S. P., & Winske, D. 1999, *JGR*, **104**, 4657
Feldman, W. C., Asbridge, J. R., Bame, S. J., & Montgomery, M. D. 1973, *JGR*, **78**, 2017
Feldman, W. C., Asbridge, J. R., Bame, S. J., & Montgomery, M. D. 1974, *RvGeo*, **12**, 715
Gary, S. P. 1991, *SpSR*, **56**, 373
Gary, S. P., McKean, M. E., & Winske, D. 1993, *JGR*, **98**, 3963
Gary, S. P., Yin, L., Winske, D., & Reisenfeld, D. B. 2000, *JGR*, **105**, 20989
Goldstein, B. E., Neugebauer, M., Zhang, L. D., & Gary, S. P. 2000, *GeoRL*, **27**, 53
Goodrich, C. C., & Lazarus, A. J. 1976, *JGR*, **81**, 2750
Gosling, J. T., Bame, S. J., Feldman, W. C., et al. 1984, *JGR*, **89**, 5409
Gray, P. C., Smith, C. W., Matthaeus, W. H., & Otani, N. F. 1996, *GeoRL*, **23**, 113
Hollweg, J. V., & Isenberg, P. A. 2002, *JGR*, **107**, 1147
Kohl, J. L., Noci, G., Antonucci, E., et al. 1998, *ApJL*, **501**, L127
Li, X., Habbal, S. R., Kohl, J. L., & Noci, G. 1998, *ApJL*, **501**, L133
Li, X., & Lu, Q. M. 2010, *JGR*, **115**, A08105

- Lu, Q. M., & Chen, L. 2009, *ApJ*, 704, 743
- Lu, Q. M., Du, A., & Li, X. 2009, *PhPl*, 16, 042901
- Marsch, E. 1991, in *Physics of the Inner Heliosphere, Vol. 2, Particles, Waves and Turbulence*, ed. R. Schwenn & E. Marsch (New York: Springer), 45
- Marsch, E. 2006, *LRSP*, 3, 1
- Marsch, E., & Livi, S. 1987, *JGR*, 92, 7263
- Marsch, E., Muhlhauer, K. H., Schwenn, R., et al. 1982, *JGR*, 87, 52
- Ofman, L., Balikhin, M., Russell, C. T., & Gedalin, M. 2009, *JGR*, 114, A09106
- Quest, Q. B. 1988, *JGR*, 93, 9649
- Richardson, J. D., Phillips, J. L., Smith, C. W., & Gary, P. C. 1996, *GeoRL*, 23, 3259
- Tu, C.-Y., Marsch, E., & Qin, Z.-R. 2004, *JGR*, 109, A05101
- Valentini, F., Califano, F., & Veltri, P. 2010, *PhRL*, 104, 205002
- Valentini, F., & Veltri, P. 2009, *PhRL*, 102, 225001
- von Steiger, R., Geiss, J., Gloeckler, G., & Galvin, A. B. 1995, *SpSR*, 72, 71
- von Steiger, R., Schwadron, N. A., Fisk, L. A., et al. 2000, *JGR*, 105, 27217
- von Steiger, R., & Zurbuchen, T. H. 2006, *GeoRL*, 33, L09103
- Winske, D. 1985, *SpSR*, 42, 53
- Winske, D., & Omidi, N. 1993, in *Computer Space Physics: Simulation Techniques and Software*, ed. H. Matsumoto & Y. Omura (Tokyo: Terra Sci.), 103